International Journal of
INTELLIGENT SYSTEMS AND APPLICATIONS IN ENGINEERING
ISSN:2147-6799 www.ijisae.org Original Research Paper

Effect of Non-Newtonian Convective Unsteady MHD Flow of Fluids on an Inclined Plate in a Porous Medium with Boundary Slip and Heat Source

Rajni[1*], Monika Kalra[2]

Submitted: 06/02/2024 **Revised**: 14/03/2024 **Accepted**: 20/03/2024

Abstract: In this research paper I have calculated and computed some of the important aspects of Impact of Convective, Unsteady MHD Flow of Fluids having Non-Newtonian Character, on Inclined Plate in a Medium of Porous Nature, with Boundary Slip, Including Heat Source. The theme of this research paper is to investigate non- Newtonian character on porous material plate in inclined position with the slip condition. The motive of investigation of this research paper is to find out certain rare results for the fluid dynamics. The problem has been solved analytically using mat lab by solving various equations culminating through process. Velocity, temperature, skin friction values/ profiles have been obtained in the wake of non-dimensional parameters such as magnetic, permeability including heat source along with Prandtl and Grashof number The present problem deals with non-Newtonian unsteady, electrically conducting fluid MHD, convective flow, on Semi-infinite, inclined plate of porous material, held in oscillating position in porous medium, with suction, over which the fluid is allowed to flow while a transverse magnetic field acted on it and velocity slip condition applied on it at the boundary. It will help the researchers for future research and experiments with different non-Newtonian fluids to find impact of slip flow using plate in inclined position.

Keywords: *Fluid dynamics, temperature, magnetic field, Flow, Non- Newtonian, Convective, Magnetohydrodynamic, Medium, Porous, Heat flux, Suction.*

1. Introduction

In recent years, there has been a growing recognition of the significance of non-Newtonian fluids in various engineering, technical, and mathematical domains. Researchers are increasingly drawn to the study of these fluids, characterized by non-conformity to conventional viscosity laws and the manifestation of non-linear relationships between elastic properties (stress and strain rate). The exploration of such fluids has garnered considerable attention, with mathematicians and physicists delving into the intricacies of their behavior. In this realm of research, numerous models have been employed, each playing a pivotal role, yet no singular model has emerged as an all-encompassing solution. The application of slip conditions, particularly in manufacturing processes, has proven to be highly effective. Notably, the implementation of increased velocity slip at the boundary has been associated with heightened heat transfer. The study at hand focuses on magnetohydrodynamic (MHD) flow within a viscoelastic, free convective fluid undergoing chemical reactions with a heat source. Yoshimura and Prud 'homme (1988) focused on providing wall slip corrections for Couette and parallel disk viscometers. Their results may include theoretical formulations or experimental data regarding slip velocity profiles and their correction methods[1]. Abbas et al. (2009) conducted an analysis of slip effects and heat transfer in a viscous fluid over an oscillatory stretching surface. Their results likely include insights into the influence of slip, oscillatory motion, and heat transfer on the flow behaviour and temperature distribution[2]. Fang and Aziz (2010) investigated viscous flow with second-order slip velocity over a stretching sheet, providing insights into the behaviour of fluids with slip effects in such scenarios [3]. Sahoo (2010) studied the effects of slip, viscous dissipation, and Joule heating on MHD flow and heat transfer of a second-grade fluid past a radially stretching sheet, highlighting the influence of various physical factors on fluid behaviour in MHD systems[4]. Fang et al. (2010) examined slip magnetohydrodynamic viscous flow over a permeable shrinking sheet, shedding light on the interplay between slip effects and magnetohydrodynamics in porous media[5].Fang et al. (2010) studied viscous flow over a shrinking sheet with a second-order slip flow model, contributing further understanding to the dynamics of shrinking surfaces with slip boundary conditions[6]. Turkyilmazoglu (2011) analytically studied heat and mass transfer of mixed hydrodynamic/thermal slip MHD viscous flow over a stretching sheet, contributing to the understanding of coupled heat and mass transfer in MHD flows with slip

[1*]*Research Scholar, Department of Mathematics, Chandigarh University, Gharuan, Mohali. ssssrjs@gmail.com.*
[2]*Associate Professor, Department of Mathematics, Chandigarh University, Gharuan, Mohali. Monika.kalra01@gmail.com.*

boundary conditions[7].Turkyilmazoglu (2011) investigated multiple solutions of heat and mass transfer of MHD slip flow for viscoelastic fluid over a stretching sheet, offering insights into the complex behaviour of viscoelastic fluids under MHD and slip conditions[8]. Sandeep, Reddy, and Sugunamma (2012) investigated the influence of radiation and chemical reaction on the transient magnetohydrodynamic (MHD) free convective flow over a vertical plate through porous media. Overall, the study elucidates the complex interplay between radiation, chemical reaction, transient effects, MHD, and porous media in convective flows over vertical plates. These findings contribute to a better understanding of heat and mass transfer processes in porous media systems, with implications for diverse fields such as environmental engineering, materials processing, and thermal management[9]. Nandeppanavar et al. (2013) analyzed MHD flow and heat transfer over a stretching surface with variable thermal conductivity and partial slip, providing understanding on how variable properties and slip conditions affect MHD flows [10]. Mukhopadhyay (2013) studied slip effects on MHD boundary layer flow over an exponentially stretching sheet with suction/blowing and thermal radiation. The findings probably reveal the impact of slip, magnetic field, suction/blowing, and radiation on the flow and heat transfer characteristics[11]. Dharmaiah Gurram, Vedavathi Nallapati, K.S. Balamurugan(2013).This paper explores the effects of radiation, chemical reaction, and Soret (thermal diffusion) on unsteady MHD free convective flow over a vertical porous plate.The study investigates how these additional factors impact the flow and heat transfer characteristics compared to the case without them[12]. Sreenivasulu et al. (2015) investigated the thermal radiation effects on magnetohydrodynamic (MHD) boundary layer slip flow over a permeable exponential stretching sheet, considering Joule heating and viscous dissipation. The results likely discuss how these factors influence the flow characteristics, such as velocity, temperature, skin friction, and heat transfer rate [13].Khader and Megahed (2015) investigated boundary layer flow due to a stretching sheet with variable thickness and slip velocity. The results probably discuss the effects of sheet thickness variation and slip velocity on the flow characteristics such as velocity profiles, skin friction, and boundary layer thickness [14]. K.S. Balamurugan, Dharmaiah Gurram, S.V.K. Varma, V.C.C. Raju (2016).The study investigates MHD free convective flow past a semi-infinite vertical permeable moving plate with heat absorption. It examines how the movement of the plate, magnetic field, and heat absorption affect the flow and heat transfer characteristics[15]. Ch. Baby Rani, Dharmaiah Gurram, K.S. Balamurugan, Sk. Mohiddin Shaw (2016). This paper discusses the synthetic response and radiation impacts on unsteady MHD free convective flow over a vertical permeable plate. It investigates how synthetic response (artificial or computational) and radiation influence the flow dynamics and heat transfer [16]. Babu et al.(2016).With buoyancy and current effect existing, heat absorbing, boundary layer, Non-Newtonian, MHD flow over porous type vertical plate, semi-infinite in nature has been examined**[17].** Sridhar et al.(2020) investigated MHD buoyancy ratio flow with radiation absorption and diffusion-thermo effects in a slip flow regime, highlighting the impact of multiple physical phenomena on fluid behaviour[18]. Vishalakshi et al. (2022) examined MHD fluid flow over a porous stretching/shrinking sheet with slips and mass transpiration, providing insights into the interplay between porous media, magnetohydrodynamics, and slip effects[19] Mahabaleshwar et al. (2023) explored the combined effects of magnetohydrodynamics and radiation on axisymmetric flow of non-Newtonian fluid past a porous shrinking/stretching surface, offering insights into complex fluid dynamics under various influences[20].

2 Mathematical Solution of the Problem & Analysis

2.1 Mathematical formulation :-

We're examining the flow of a fluid that can't be compressed, and it's moving due to convection. This fluid doesn't follow typical Newtonian viscosity laws, and it conducts electricity. We're studying how this fluid behaves when it flows past a flat surface that's tilted at an angle (∅) relative to the flow direction. This surface is immersed in a fluid at temperature T∞, and it's situated in a porous medium.Now, imagine a magnetic field (B0) that's perpendicular to this surface. We're using a Cartesian coordinate system to describe positions and terms. The X-axis points in the direction of the plate's movement, while the Y-axis points perpendicular to the plate.We're interested in two components of velocity: u, which is in the direction of the X-axis (parallel to the plate's movement), and v, which is in the direction of the Y-axis (perpendicular to the plate).Now, considering physical quantities like velocity, temperature, and so on, we'll express them as functions of y (position along the Y-axis) and t (time). We're assuming that the Reynolds number, which characterizes the ratio of inertial forces to viscous forces, is very small. Also, we're assuming that any induced magnetic field effects are negligible, and we're treating pressure as constant throughout the flow. Additionally, at the plate's surface, there's a suction effect with velocity (-V), meaning the fluid is being drawn into the plate.

Continuity Equation is given below

$\frac{\partial u}{\partial y}=0$ …… (1)

$\frac{\partial u}{\partial t} - V\frac{\partial u}{\partial y} = (\nu + \alpha\frac{\partial}{\partial t})\frac{\partial^2 u}{\partial y^2} + g\beta(T-T_\infty)cos\emptyset - \frac{\nu}{K_0}u - \frac{\sigma {B_0}^2 u}{\rho}$ ……. (2)

$\frac{\partial T}{\partial t} - V\frac{\partial T}{\partial y} = k\,[1+\alpha\frac{\partial}{\partial t}]\frac{\partial^2 T}{\partial y^2} - S[\,T - T_\infty]$ …. . (3)

Boundary conditions are

y = 0: u= L $[\frac{\partial u}{\partial y}]$, T = $T_\infty + (T_\omega - T_\infty)\, e^{i\omega t}$]

y→∞ : u →V_0, T→ T_∞] …… (4)

terms used above are specified; k denotes thermal diffusivity, α used for stress moduli, velocity component of flow as u in the direction-x, g denotes gravitational force, porous medium permeability K_0, density ρ, ν for kinematic viscosity, β specifies volumetric heat transfer expansion coefficient, S for heat source parameter, T_∞ symbolises fluid temperature remote from the plate, T for temperature, L is slip parameter, ∅ for angle of inclination of plate, transverse magnetic field is B_0, σdenotes electrical conductivity and ω symbolises frequency of oscillation.

2. 2 Deriving dimensionless quantities

$\mathbf{u^*}=\frac{u}{V_0}t^* = \frac{t{V_0}^2}{\nu}$ $\boldsymbol{\theta} = \frac{T-T_\infty}{T_\omega - T_\infty}\boldsymbol{\omega}^* = \frac{\nu\omega}{{V_0}^2}\boldsymbol{y}^* = \frac{yV_0}{\nu}\boldsymbol{\alpha}^* = \frac{\alpha {V_0}^2}{\nu}$

$s^*=\frac{\nu S}{{V_0}^2}V^* = \frac{V}{V_0}$ $\boldsymbol{h} = \frac{V_0 L}{\nu}\boldsymbol{K_p} = \frac{k_0 {V_0}^2}{\nu^2}\frac{k}{\nu} = \frac{1}{P_r}\mathbf{M^2}=\frac{\sigma {B_0}^2 \nu}{\rho {\nu_0}^2}$

$\mathbf{G_r}=\nu g\beta\frac{T_\omega - T_\infty}{{V_0}^3}$

P_rPrandtl number,M Hartman number and G_r stand Grashof number.

Equations (2), (3) and boundary condition at(4) reduce to,

$\frac{\partial u^*}{\partial t^*} - V^*\frac{\partial u^*}{\partial y^*} = \frac{\partial^2 u^*}{\partial y^{*2}} + \alpha^*\frac{\partial^3 u^*}{\partial t^* \partial y^{*2}} + G_r\theta cos\emptyset - \frac{1}{K_p}u^* - M^2 u^*$ …… (5)

$\frac{\partial \theta}{\partial t^*} - V^*\frac{\partial \theta}{\partial y^*} = \frac{\kappa}{\upsilon}\frac{\partial^2 \theta}{\partial y^{*2}} + \frac{\kappa}{\upsilon}\alpha^*\frac{\partial^3 \theta}{\partial t^* \partial y^{*2}} - S^*\theta$ …… (6)

Emerging boundary conditions are

y^* =0 , $u^*= h[\frac{\partial u^*}{\partial y^*}]$,$\theta= e^{i\omega t}$…… . (7)

$y^* \to \infty$, $u^* \to 1$, $\theta \to 0$

Solving thee equations

Dropping (*)and solving non-linear partial differential equation (5), (6) including boundary condition (7),

u = $U_0(y) + U_1(y)e^{i\omega t}$ …… …… (8)

$\theta = T_0(y) + T_1(y)e^{i\omega t}$ … …… (9)

U_0, U_1, T_0,T_1 , represent functions of y and U_0 , U_1, T_0,$T_1$to be determined.

Taking values of u and θ from equations (8), (9) and putting in equation (5),

culminating equations are :-

$$\frac{d^2U_0}{dy^2} - V\frac{dU_0}{dy} - (\frac{1}{K_p} + M^2)\,U_0 = -G_r T_0 cos\emptyset \ldots \quad (10)$$

$$\frac{d^2U_1}{dy^2} + \frac{V}{1+\alpha i\omega}\frac{dU_1}{dy} - \frac{\frac{1}{K_p}+M^2+i\omega}{1+\alpha i\omega}U_1 = \frac{-G_r T_1 cos\emptyset}{1+\alpha i\omega} \ldots \quad (11)$$

$$\frac{d^2T_0}{dy^2} + VP_r\frac{dT_0}{dy} + SP_rT_0 = 0 \ldots \quad (12)$$

$$\frac{d^2T_1}{dy^2} + \frac{VP_r}{(1+\alpha i\omega)}\frac{dT_1}{dy} + \frac{(S-i\omega)P_r}{(1+\alpha i\omega)}T_1 = 0 \ldots \quad (13)$$

After calculation boundary conditions come out to be,

At y=0 $T_0(0)=0$, $T_1(0)=1$, $U_0(0)=h[\frac{dU_0}{dy}]$, $U_1(0)=h[\frac{dU_1}{dy}]$… (14)

At y→ ∞ $T_0 \to 0$, $T_1 \to 0$, $U_0 \to 1, U_1 \to 0$……… .(15)

Equation (12),(13) along with boundary equations (14) and (15) yield the following result.

$T_0(y) = 0$ …………………… … (16)

$T_1(y) = \exp.(-P_4 y)$ ……………………………………… (17)

Where $P_4 = \frac{D_1+\sqrt{{D_1}^2-4D_2}}{2}$, $D_1 = \frac{VP_r}{(1+\alpha i\omega)}$, $D_2 = \frac{(S-i\omega)P_r}{(1+\alpha i\omega)}$

Putting the above result, equations (16) and (17) in equation (10) and (11),second order differential equations are yielded. Applying here boundary conditions as in equation (14) and (15), it gives

$$\frac{d^2U_0}{dy^2} - V\frac{dU_0}{dy} - (\frac{1}{K_p} + M^2)\,U_0 = 0 \ldots \quad (18)$$

$$\frac{d^2U_1}{dy^2} + \frac{V}{1+\alpha i\omega}\frac{dU_1}{dy} - \frac{\frac{1}{K_p}+M^2+i\omega}{1+\alpha i\omega}U_1 = \frac{-G_r cos\emptyset}{1+\alpha i\omega}\ \exp.(-P_4 y) \ldots \quad (19)$$

$$U_0(y) = \exp(P_5 y) + \frac{(hP_5-1)}{(1+hP_6)}\exp(-P_6 y) \ldots \quad (20)$$

$$U_1(y) = C_8\exp(-P_8 y) + \frac{D_5}{({P_4}^2-P_4D_3-D_4)}\exp(-P_4 y) \ldots \quad (21)$$

Where $C_8 = \frac{-D_5(1+hP_4)}{(1+hP_8)({P_4}^2-P_4D_3-D_4)}$

Where $P_8 = \frac{D_3+\sqrt{{D_3}^2+4D_4}}{2}, D_3 = \frac{V}{1+\alpha i\omega,}, D_4 = \frac{\frac{1}{K_p}+M^2+i\omega}{1+\alpha i\omega}, D_5 = \frac{-G_r cos\emptyset}{1+\alpha i\omega}$

Now values of U_0,$U_1$and $T_0, T_1$are put in equation (8) and (9), where by it yields.

$$u = \exp(P_5 y) + \frac{(hP_5-1)}{(1+hP_6)}\exp(-P_6 y) + (C_8\exp(-P_8 y) + \frac{D_5}{({P_4}^2-P_4D_3-D_4)}\exp(-P_4 y))e^{i\omega t} \ldots \quad (22)$$

$$\theta = = \exp.(-P_4 y)\ e^{i\omega t} \ldots \quad (23)$$

3 Results & findings

This research delves into the intricate realm of fluid dynamics, particularly focusing on the behavior of non-Newtonian fluids as they flow through porous media. The study investigates a complex scenario involving convective, electrically conducting, magnetohydrodynamic flow past an inclined porous plate. Notably, the analysis incorporates slip effects near the boundary and considers the influence of a transverse magnetic field on the semi-infinite oscillatory flow. Pr=1, M=2, V=4, Kp=0.5, S=0.5, alpha=0.3, Phi=pi/6, exp.=2.7183, w=0.2,t=0.5,h=0.01.The primary objective is to analytically derive expressions for the velocity and temperature profiles, accounting for various parameters' effects. Parameters such as Prandtl number (Pr), magnetic field strength (M), permeability (Kp), slip parameter (S), and the angle of inclination (Φ) are systematically examined to understand their impact on the flow dynamics. The results provide insights into how these factors shape the flow behavior.

In Table-1, the study elucidates the influence of different parameters on skin friction (Cf). Notably, an increase in Grashof number (Gr) and magnetic field strength (M) correlates with heightened skin friction. Conversely, an increase in Prandtl number (Pr), permeability (Kp), normal stress moduli (α), and angle of inclination (Φ) leads to a decrease in skin friction.

Table-2 sheds light on the Nusselt number (Nu), a dimensionless parameter characterizing the heat transfer rate. The analysis reveals that an increase in the heat source parameter (S) corresponds to an increase in Nu, while an increase in Prandtl number (Pr) results in a decrease. Moreover, Nu decreases with increasing suction velocity (V) but increases with higher values of normal stress moduli (α).

Tables 3 and 4 facilitate a comparison between the study's findings and those of previous research, particularly referencing Babu et al. (2018). This comparative analysis validates the accuracy and reliability of the obtained results, particularly concerning skin friction and Nusselt number.

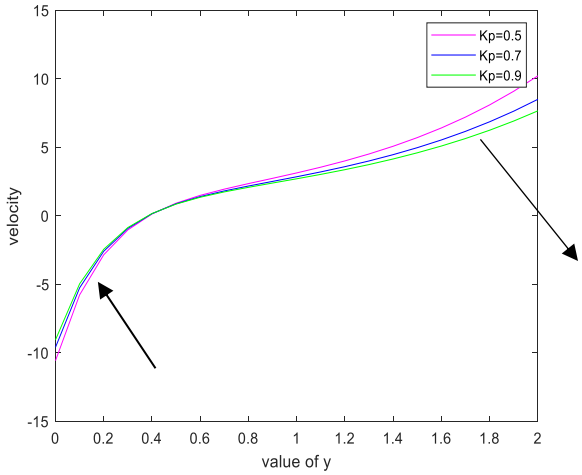

Fig. 1.Represents Permeability parameter for Velocity profile

Fig. 1, the velocity profile exhibits an intriguing behaviour when plotted against the permeable parameter, with a noticeable increase as the parameter varies. In Figure 1, there's a point of intersection around 0.5, after which the velocity gradually decreases as it moves away from the permeable plate. This trend highlights the dynamic relationship between velocity and the permeable parameter, showcasing how certain values lead to heightened velocities while others result in a gradual decline.

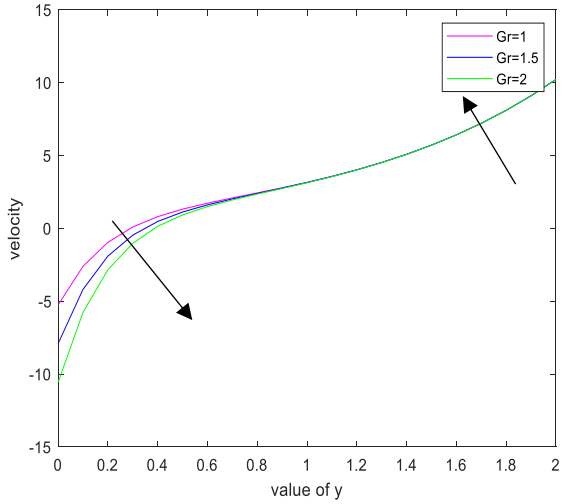

Fig. 2. Represents Grashof Number for Velocity profile.

Fig. 2, The velocity profile (u) plotted against the distance from the permeable plate (y) reveals an intriguing trend when considering varying values of the Grashof number (Gr). Initially, as the Grashof number increases, the velocity decreases. This phenomenon is clearly observed in the plotted figure. Interestingly, there exists a point, approximately around 0.5 on the Grashof number scale, where the velocity curves intersect. Beyond this point, as the Grashof number continues to increase, the velocity profile begins to exhibit an increase.To elaborate on this result, let's consider the physical implications. The Grashof number represents the ratio of buoyancy forces to viscous forces in a fluid flow system. When the Grashof number is small, viscous forces dominate, resulting in a slower velocity profile near the permeable plate. However, as the Grashof number increases, buoyancy forces become more significant, leading to a decrease in velocity. This decrease continues until a critical point, around Gr = 0.5, where the effects of buoyancy and viscous forces balance out, causing the velocity profiles to intersect.Beyond Gr ≈ 0.5, buoyancy forces increasingly dominate, surpassing the influence of viscous forces. Consequently, the velocity profile experiences an upsurge as the Grashof number increases further away from the permeable plate. This behavior reflects the intricate interplay between buoyancy and viscous forces in the fluid flow near a permeable surface, highlighting the importance of considering both parameters in understanding and predicting the velocity distribution in such systems.

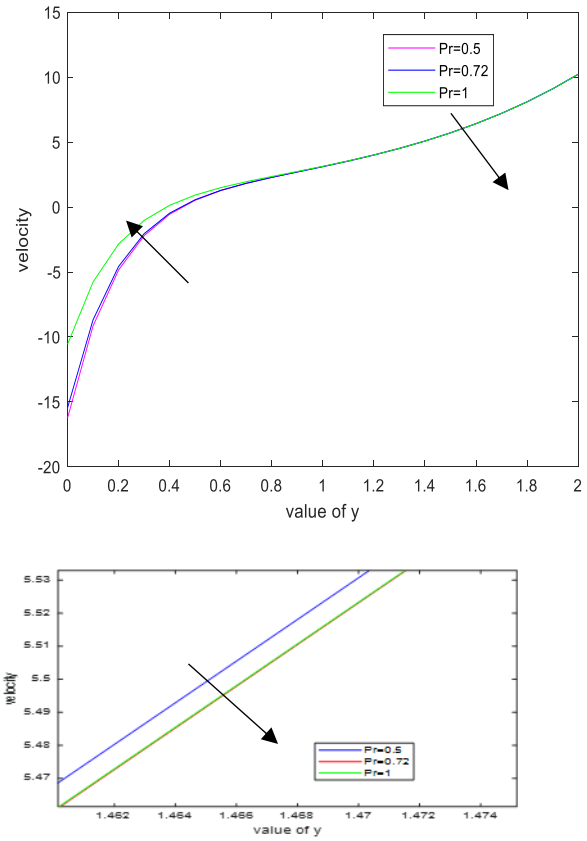

Fig. 3, the velocity profile plotted against distance from a permeable plate shows an interesting trend with varying Prandtl numbers (Pr). As Prandtl number increases, the velocity initially rises, reaching an intersection point around 0.5 distance from the plate. Beyond this point, the velocity gradually decreases as the distance from the plate increases. This behavior suggests a dynamic relationship between Prandtl number and velocity distribution near the plate, with higher Prandtl numbers resulting in enhanced velocities initially before tapering off further away.

Fig. 3. Represents Prandtl Number for Velocity profile.

Fig. 4, the plot shows how velocity (u) changes with distance from a permeable plate (y), with different levels of a heat source parameter (S). As S increases, the velocity curve initially decreases until around 0.5, where intersections occur. Beyond this point, as y increases further from the plate, the velocity profile starts to rise again. This suggests that the impact of the heat source on velocity is most pronounced near the plate, gradually diminishing as distance from the plate increases.

Fig. 4. Represents Heat source parameter for Velocity

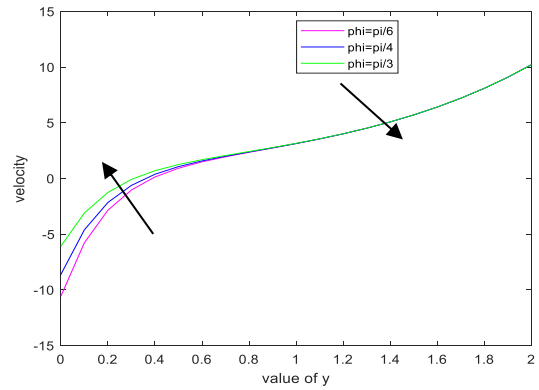

Fig. 5, exhibit velocity, u plotted against y, varying values of Phi, the angle of inclination, help tracing velocity curve. It increases and it is seen in the figure 5 that at near about 0.5 they intersect and as it goes far from the permeable plate velocity profile decreases.

Fig. 5. Represents Angle of inclination for velocity profile.

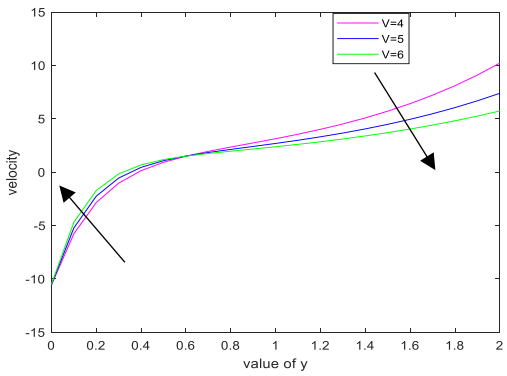

Fig. 6. Represents Suction Velocity for velocity profile.

Fig. 6, in the plotted velocity profile of velocity (u) against distance from the permeable plate (y), it's observed that varying values of suction velocity (V) produce distinct velocity curves. Initially, as the distance from the plate increases (y), the velocity (u) increases, indicating the acceleration of the fluid. At approximately y = 0.5, there is an intersection point where different suction velocities intersect. Beyond this point, as y further increases, the velocity profile gradually decreases. Near the permeable plate, the suction velocity (V) induces a flow towards the plate, causing an increase in velocity (u) as we move away from the plate. This acceleration is due to the suction effect drawing fluid towards the plate. The intersection point signifies a balance between the suction velocity (V) and the tendency of the flow to dissipate away from the plate. At this point, the effect of suction is still strong enough to maintain a relatively high velocity, but as y increases further, the suction effect diminishes. Beyond the intersection point, the suction effect weakens with increasing distance from the plate. Consequently, the velocity profile gradually decreases as the flow transitions from being influenced predominantly by suction to the natural tendency of the fluid to disperse.Varying the suction velocity (V) alters the intensity of the suction effect near the plate, thereby affecting the shape and magnitude of the velocity profile. Higher suction velocities result in a more pronounced acceleration near the plate and a steeper velocity profile, while lower suction velocities lead to a more gradual change in velocity.

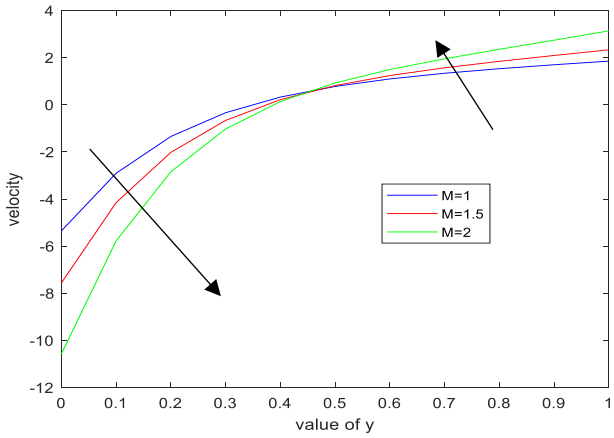

Fig. 7 Represents Magnetic Parameter for velocity profile.

Fig. 7. When examining the velocity plotted against the distance from the permeable plate (y), with the Magnetic parameter (M) as a variable, a distinct trend emerges. Initially, the velocity decreases, forming a curve. Notably, around a Magnetic parameter value of approximately 0.5, there's a notable intersection in the velocity curves. However, as the distance from the permeable plate increases, the velocity profile begins to ascend, indicating an increase in velocity away from the plate.

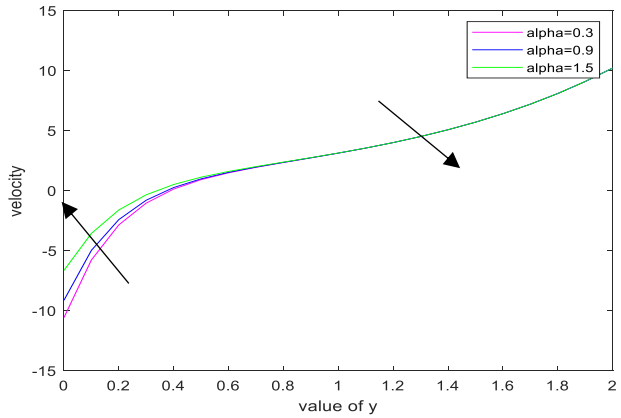

Fig. 8, The velocity profile exhibits an increasing trend when plotted against the distance from the permeable plate, represented by the variable \(y \), for varying values of alpha and Normal Stress Moduli. In the plotted curve, there is a distinct point, approximately at \(y \approx 0.5 \), where the velocity profiles intersect. Beyond this point, as the distance from the permeable plate increases, the velocity gradually decreases, forming a characteristic figure-eight pattern.

Fig. 8. Represents Normal Stress moduli alpha for velocity profile.

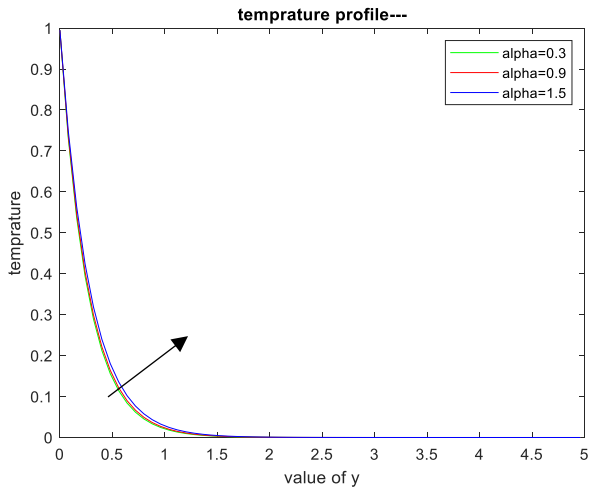

Fig.9. Sharp increase in temperature with increasing y. This suggests that there's some heat generation or transfer mechanism that becomes more significant as you move along the y-axis. It could be due to friction, chemical reactions, or some other physical process that generates heat. For example, if you're dealing with a system where friction plays a role, as y increases, there might be more surface interaction leading to more frictional heat generation. Increase in temperature magnitude with increasing α. The Normal Stress modulus (α) likely influences the system's thermal behavior. A higher α could indicate either a material with greater thermal conductivity or a material that generates more heat under stress. In either case, as α increases, more heat is either conducted or generated within the system, leading to a higher temperature. Overall, the observed result indicates a complex interplay between mechanical stress (manifested by y and α) and thermal effects (manifested by θ). This could be crucial in understanding and predicting the thermal behavior of systems subjected to mechanical stress, with practical applications in various engineering fields like materials science, civil engineering, or mechanical engineering.

Fig. 9. Represents Normal Stress Moduli alpha for Temperature Profil

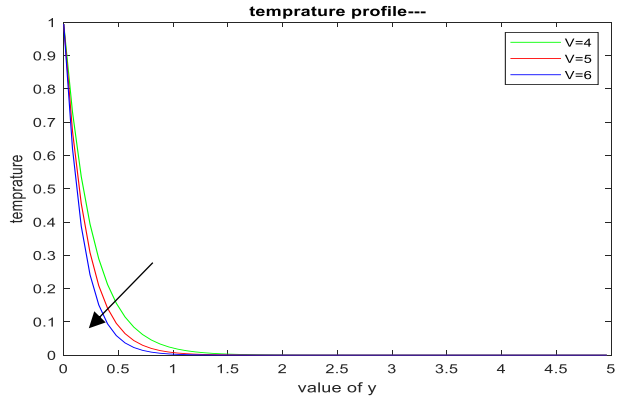

Fig. 10. The temperature profile relative to suction velocity illustrates how different suction velocity values affect the temperature curve. As the distance from the boundary layer decreases (approaching the plate), there's a notable rapid decline in temperature towards zero. This decrease corresponds to an increase in suction velocity, particularly in close proximity to the plate.

Fig. 10. Represents Suction Velocity for Temperature Profile.

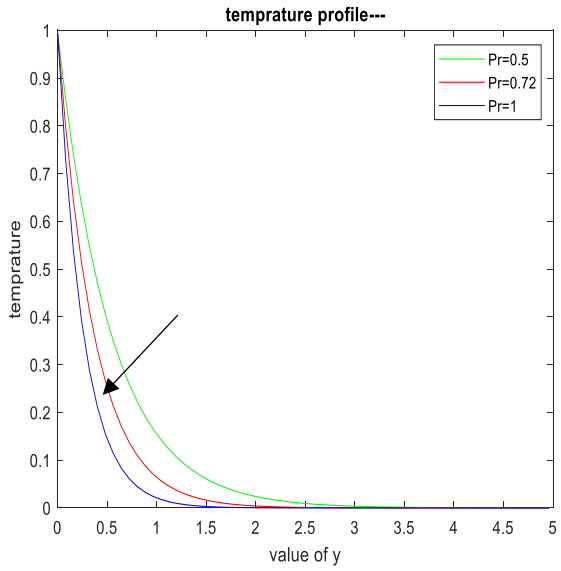

Fig. 11. Represents Prandtl Number for Temperature Profile

Fig.11 The temperature profile, influenced by the Prandtl number (Pr), manifests distinct characteristics as Pr varies. By exploring a range of Pr values, we can discern the trajectory of the temperature curve. Notably, as the y-coordinate increases, a significant and rapid decline in the temperature profile occurs, ultimately approaching zero.This phenomenon merits a closer examination. The Prandtl number serves as a measure of the relative rates of momentum and thermal diffusion within a fluid. A higher Prandtl number signifies that thermal diffusivity is relatively weaker compared to momentum diffusivity, indicating a reduced efficiency in heat transfer relative to momentum transfer.As Pr increases, the temperature profile exhibits a sharper decrease along the y-axis. This indicates that the rate of heat dissipation diminishes more rapidly with increasing y-values. Essentially, thermal diffusion becomes less effective compared to momentum diffusion, leading to a more pronounced temperature gradient.The observed convergence of the temperature profile towards zero as y increases reflects the diminishing influence of thermal diffusion. In scenarios where the Prandtl number tends towards infinity, signifying an overwhelming dominance of momentum diffusivity over thermal diffusivity, the temperature gradient approaches zero asymptotically. This suggests a scenario where the temperature distribution becomes increasingly uniform with minimal variation along the y-axis.

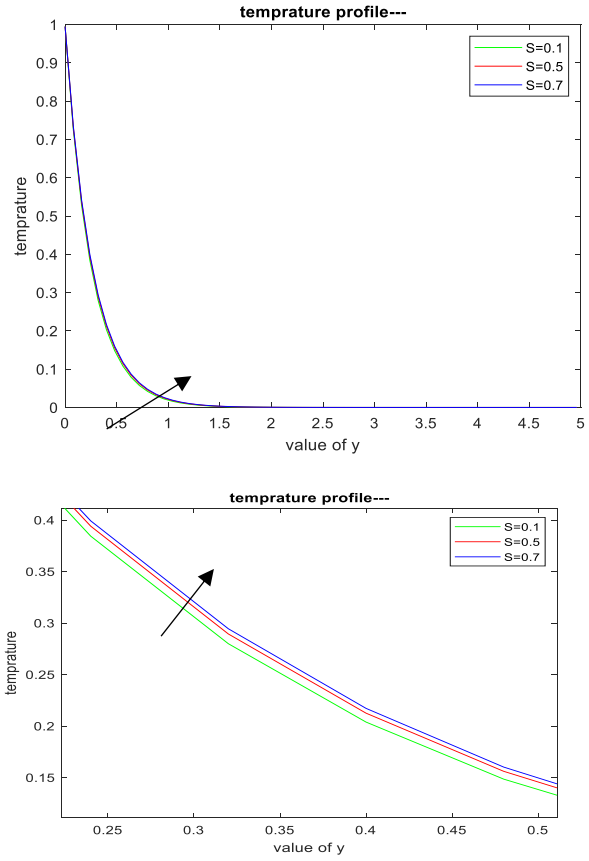

Fig. 12. Represents Heat source parameter for Temperature Profile.

Fig. 12 The temperature profile in relation to the Heat Source parameter demonstrates how different values of S influence the temperature curve. As the Heat Source parameter increases, the temperature field θ exhibits a sharp decline near the boundary before eventually approaching zero. Elevated S values near the plate correspond to a notable decrease in θ. This observation underscores the significant role of the Heat Source parameter in shaping the temperature distribution, particularly near the boundary, and highlights its impact on the thermal behavior of the system.

4 Mathematical Findings

Skin Friction (C_f) at the plate

$$C_f = [\frac{\partial u}{\partial y}]_{y=0} = (P_5) + \frac{(hP_5-1)}{(1+hP_6)}(-P_6)+(C_8(-P_8) + \frac{D_5}{({P_4}^2-P_4D_3-D_4)}(-P_4))e^{i\omega t} \quad \ldots\ldots\ldots\ldots \quad (24)$$

Table 1. Computed values of C_f displayed hereunder

S	Gr	Pr	Kp	V	alpha	Phi	M	C_f
0.5	2	1	0.5	4	0.3	$\pi/6$	2	61.08687
0.1	2	1	0.5	4	0.3	$\pi/6$	2	57.55308
0.7	2	1	0.5	4	0.3	$\pi/6$	2	62.84707
0.5	1	1	0.5	4	0.3	$\pi/6$	2	33.55048
0.5	1.5	1	0.5	4	0.3	$\pi/6$	2	47.31868
0.5	2	0.5	0.5	4	0.3	$\pi/6$	2	90.54890
0.5	2	0.72	0.5	4	0.3	$\pi/6$	2	86.33002
0.5	2	1	0.7	4	0.3	$\pi/6$	2	55.00399
0.5	2	1	0.9	4	0.3	$\pi/6$	2	51.67558
0.5	2	1	0.5	5	0.3	$\pi/6$	2	70.33532
0.5	2	1	0.5	6	0.3	$\pi/6$	2	79.88965
0.5	2	1	0.5	4	0.9	$\pi/6$	2	52.56448
0.5	2	1	0.5	4	1.5	$\pi/6$	2	38.60111
0.5	2	1	0.5	4	0.3	$\pi/4$	2	50.98083
0.5	2	1	0.5	4	0.3	$\pi/3$	2	37.81038
0.5	2	1	0.5	4	0.3	$\pi/6$	1	30.43883
0.5	2	1	0.5	4	0.3	$\pi/6$	1.5	42.82953

5 Coefficient of Heat Transfer

Mathematically,

$$Nu = [\frac{\partial \theta}{\partial y}]_{y=0} = (-P4)e^{i\omega t} \ldots\ldots\ldots\ldots\ldots\ldots \quad (25)$$

Table 2. Values of Nu computed, displayed hereunder.

S	Pr	V	alpha	Nu
0.5	1	4	0.3	-3.8404
0.1	1	4	0.3	-3.9437
0.7	1	4	0.3	-3.7865
0.5	0.5	4	0.3	-1.8530
0.5	0.72	4	0.3	-2.7283
0.5	1	5	0.3	-4.8581
0.5	1	6	0.3	-5.8666
0.5	1	4	0.9	-3.7360
0.5	1	4	1.5	-3.5384

Table 3. Comparison of different values of Pr for Skin friction

Pr	**Babu[17]**	**Present Study**
0.71	0.039855	15.651260
3	0.048555	15.572905
7	0.051454	15.555354

Table 4. Comparison of different values of Pr for Nusselt Number

Pr	Babu[17]	Present Study
0.71	-0.733466	-0.2331909
3	-3.059900	-0.2834332
7	-7.123040	-0.2976734

6. Conclusion

In this research paper we have concluded regarding the tables and graphs which have been mentioned above mathematical findings are as follows -

1. As the magnetic parameter (M), heat source parameter (S), suction velocity (V), and Grashof number (Gr) increase, there is a successive rise in the skin-friction coefficient (Cf). This suggests that higher values of these parameters lead to increased frictional forces exerted by the fluid on the surface.
2. Increasing the permeable parameter (Kp), normal stress moduli alpha, and Prandtl number (Pr) results in a decrease in the skin-friction coefficient (Cf). This implies that greater permeability, normal stress, and Prandtl number contribute to reduced frictional forces between the fluid and the surface.
3. When the Prandtl number (Pr) and normal stress moduli alpha increase, there is a concurrent decrease in both the Nusselt number and the temperature field θ. This indicates that higher Prandtl numbers and normal stress moduli lead to reduced heat transfer and temperature distribution within the fluid.
4. An increase in the heat source parameter (S), coupled with suction velocity V, leads to an increase in both the Nusselt number and the temperature field θ. This suggests that higher heat sources and suction velocities enhance heat transfer and elevate the temperature profile within the fluid.
5. Increasing the normal stress moduli alpha and the heat source parameter (S) results in an increase in the Nusselt number. However, the velocity field of the fluid exhibits an interesting behaviour. it shows an increase near the permeable plate for normal stress moduli alpha, suction velocity (S), permeable parameter (Kp), and Prandtl number (Pr), but it decreases as the distance from the permeable plate increases. This suggests that while higher normal stress and heat sources enhance heat transfer, they also affect the fluid velocity differently depending on the proximity to the permeable plate.

References

[1] Yoshimura, A., & Prud'homme, R. K. (1988). Wall slip corrections for Couette and parallel disk viscometers. *Journal of Rheology*, *32*(1), 53-67.

[2] Abbas, Z., Wang, Y., Hayat, T., & Oberlack, M. (2009). Slip effects and heat transfer analysis in a viscous fluid over an oscillatory stretching surface. *International Journal for Numerical Methods in Fluids*, *59*(4), 443-458.

[3] Fang, T. & Aziz, A.(2010). Viscous fow with second order slip velocity over a stretching sheet. Zeitschrif Fur Naturforschung A. 65, 195–203.

[4] Sahoo, B. (2010). Effects of slip, viscous dissipation and Joule heating on the MHD flow and heat transfer of a second grade fluid past a radially stretching sheet. *Applied Mathematics and Mechanics*, *31*, 159-173.

[5] Fang, T. G., Zhang, J. & Yao, S. S.(2010). Slip magnetohydrodynamic viscous fow over a permeable shrinking sheet. Chin. Phys. Lett. 27, 124702.

[6] Fang, T., Yao, S., Zhang, J. & Aziz, A.(2010). Viscous fow over a shrinking sheet with a second order slip fow model. Commun. Nonlinear Sci. Numer. Simul. 15, 1831–1842.

[7] Turkyilmazoglu, M. (2011). Analytic heat and mass transfer of the mixed hydrodynamic/thermal slip MHD viscous flow over a stretching sheet. *International Journal of Mechanical Sciences*, *53*(10), 886-896.

[8] Turkyilmazoglu, M. (2011). Multiple solutions of heat and mass transfer of MHD slip flow for the viscoelastic fluid over a stretching sheet. *International Journal of Thermal Sciences*, *50*(11), 2264-2276.

[9] Sandeep, N., Reddy, A. V. B., & Sugunamma, V. (2012). Effect of radiation and chemical reaction on transient MHD free convective flow over a vertical plate through porous media. *Chemical and process engineering research*, *2*, 1-9.

[10] Nandeppanavar, M. M., Vajravelu, K., Subhas Abel, M., & Siddalingappa, M. N. (2013). MHD flow and heat transfer over a stretching surface with variable thermal conductivity and partial slip. *Meccanica*, *48*, 1451-1464.

[11] Mukhopadhyay, S. (2013). Slip effects on MHD boundary layer flow over an exponentially stretching sheet with suction/blowing and thermal

radiation. *Ain Shams Engineering Journal*, *4*(3), 485-491.

[12] Dharmaiah, G., & Krishna, M. V. (2013). Finite difference analysis on mhd free convection flow through a porous medium along a vertical wall. *Asian Journal of Current Engineering and Maths*, *2*(4), 273-280.

[13] Sreenivasulu, P., Poornima, T., & Bhaskar Reddy, N. (2015). Thermal radiation effects on MHD boundary layer slip flow past a permeable exponential stretching sheet in the presence of joule heating and viscous dissipation. *Journal of Applied Fluid Mechanics*, *9*(1), 267-278.

[14] Khader, M. M., & Megahed, A. M. (2015). Boundary layer flow due to a stretching sheet with a variable thickness and slip velocity. *Journal of Applied Mechanics and Technical Physics*, *56*, 241-247.

[15] Balamurugan, K. S., Gurram, D., Varma, S. V. K., & Raju, V. C. C. (2016). MHD free convective flow past a semi-infinite vertical permeable moving plate with heat absorption. *International Journal of Engineering & Scientific Research*, *4*(8), 46-58.

[16] Rani, C. B., Dharmaiah, G., Balamurugan, K., & Shaw, S. M. (2016). Synthetic response and radiation absorption impacts on unsteady mhd free convective flow over a vertical permeable plate. Int. J. Chem. Sci., 14(4), 2051-2065.

[17] Babu, D. D., Venkateswarlu, S., & Reddy, E. K. (2018). Heat and mass transfer on MHD flow of Non-Newtonian fluid over an infinite vertical porous plate with Hall effects. *International Journal of Pure and Applied Mathematics*, *119*(15), 87-103.

[18] Sridhar, W., Dharmaiah, G., Rao, D. S., & Kumar, R. D.(2020). Mhd buoyancy ratio flow in the presence of radiation absorption and diffusion-thermo effects in a slip flow regime. Journal of Xi'an University of Architecture & Technology, XII(V), 2479-2508.

[19] Vishalakshi, A. B., Mahabaleshwar, U. S., & Sarris, I. E. (2022). An MHD fluid flow over a porous stretching/shrinking sheet with slips and mass transpiration. *Micromachines*, *13*(1), 116.

[20] Mahabaleshwar, U. S., Maranna, T., Perez, L. M. & Ravichandra Nayakar, S. N.(2023). An efect of magnetohydrodynamic and radiation on axisymmetric fow of non-Newtonian fuid past a porous shrinking/stretching surface. J. Magn. Magn. Mater. 571, 170538.